Reconstructing Three-Dimensional Magnetic Structure of A Solar Active Region During its Emergence Phase Using SDO/HMI Observations

Georgios Chintzoglou and Jie Zhang

School of Physics, Astronomy and Computational Sciences, George Mason University, 4400 University Dr., MSN 6A2, Fairfax, VA 22030, USA

gchintzo@gmu.edu

ABSTRACT

A solar active region (AR) is a three dimensional magnetic structure formed in the convection zone, whose property is fundamentally important for determining the coronal structure and solar activity when emerged. However, our knowledge on the detailed 3-D structure prior to its emergence is rather poor, largely limited by the low cadence and sensitivity of previous instruments. Here, using the 45-second high cadence observations from the Helioseismic and Magnetic Imager (*HMI*) instrument onboard the Solar Dynamics Observatory (*SDO*), we are able for the first time to determine and reconstruct the detailed three-dimensional magnetic structure of NOAA AR 11158 during the emergence phase and to characterize its magnetic connectivity and topology. This task is accomplished with the aid of the image-stacking method and advanced 3-D visualization. We find that the AR consists of two major bipoles, or four major polarities. Each polarity shows interesting tree-like structure, i.e. while the bottom of the polarity appears as a single trunk-like flux-tube, the top of the polarity has multiple branches, consisting of smaller and thinner flux-tubes which connect to the branches of the opposite polarity that is similarly fragmented. The roots of the four polarities align well along a straight line, while the top branches are slightly non-coplanar. Our observations suggest that an active region, even appearing most complicated on the surface, may originate from a simple straight flux-tube that undergoes both horizontal and vertical bifurcation processes during its rise through the convection zone.

Subject headings: Sun: general — Sun: active region — Sun: magnetic field

1. Introduction

The subject of AR magnetic structure in the Solar Convection Zone (SCZ) is one of the least understood but of crucial importance for constraining solar dynamo models and explaining what drives solar activity and space weather. It is widely believed that ARs seen on the surface are magnetic flux-tubes that are being created by the dynamo process at a depth in the SCZ (Charbonneau 2005). Subsequently, the flux-tubes emerge through the photospheric surface giving birth to ARs or sunspots and magnetic loop systems in the corona. On the surface, there is a high order of regularity on the pattern of AR magnetic polarities, well described by the Hale's Law and Joy's laws (Hale et al. 1919).

There is limited information on the AR three-dimensional (3D) structure inferred from observations of AR emergence. Zwaan (1987) provided a toy-model explanation of AR emergence by attributing it to the subsurface structure of an Ω-shaped loop of magnetic flux with a frayed crest that brakes through the surface giving rise to the observed appearance of bipolar ARs. The work by Strous et al. (1996) and Strous & Zwaan (1999) extends this model to include the horizontal dynamics in order to explain the fact that many flux-tubes emerge in multiple locations. Tanaka (1991) studied complex (delta configuration) ARs that exhibit rotational proper motions during their evolution (starting from Hale's and Joy's laws incompatible towards being compatible) and attributed it to a knotted 3D topology. Also, Leka et al. (1996) found evidence that flux-tubes emerge kink-deformed by the current they carry, thus containing a twisted 3-D structure differernt from an Ω-shaped flux-tube. However, it is generally difficult to determine the detailed 3-D structure of an AR, due to the limitation of previous observations in terms of temporal and spatial resolution.

On the other hand, there has been a considerable amount of theoretical works which have been developed over the past four decades trying to attack the issue computationally (for a review, see Fan 2009). The models of emergence in the SCZ are (a) the Thin Flux Tube model (TFT, Spruit 1981) and (b) the anelastic MHD model (Gough 1969) . While both models work well in the lower SCZ, they might not be valid at the top layers of the SCZ (that is, 20 - 30 Mm below surface), as the flux-tubes are not thin (TFT assumption breaks down) and the velocity field is not subsonic (anelastic approximation breaks down). The reason for making such differences lies behind the strong pressure gradient at the layers close to the surface (Fan 2009; Stein 2012). Thus, theoretical works usually split the SCZ into two parts, the lower SCZ and the upper SCZ ($\sim 20\,\mathrm{Mm}$).

With the improvement of computational power and sophisticated algorithms, it has been possible for more "realistic" numerical experiments (i.e. fully compressible, radiative-convective 3D MHD simulations) to explore the formation of pores and sunspots (e.g. Cheung et al. 2010; also see review by Stein 2012), although the spatial domain achieved so far is still very small (the "deepest" simulations go down to a depth of 20 Mm in spite of the full size of the SCZ, ~ 220 Mm). Also, radiative-convective MHD models provide no explanation on large scale characteristics of emerging ARs – such as the Joy's law of AR tilts and asymmetric foot-point separation – which are reproducible by global-scale models, like the TFT approximation (Caligari et al. 1995) and anelastic MHD simulations (Fan 2008). To this date, because of the computational restrictions of our current era and the natural complexity of this task, there's no global, fully compressible MHD model yet capable in probing the evolution of flux emergence throughout the entire SCZ to the surface (Fan 2009).

In this letter, we present the implementation of an image-stacking technique as a mean to reconstruct and study the 3-D structure of an emerging AR directly from observations and with great detail. The NOAA AR 11158 presented in Figure 1, is known as the one that produced the very first X-class flare (X2.2) of the Solar Cycle 24 and its energetics have been studied thoroughly by Sun et al. (2012). The photospheric magnetogram images show a complex AR as seen from the surface. However, with our 3D reconstruction method, it is rather evident that AR 11158 has a much simpler origin, i.e. the horizontal and vertical bifurcation of a single progenitor flux-tube. This is probably the first such study of directly reconstructing the detailed 3-D structure and topology of solar active regions.

2. Methodology

In this study, we used high time-cadence and high spatial resolution observations ($0\farcs5$/pixel) taken by the HMI instrument on board the SDO spacecraft (Schou et al. 2012). The HMI instrument is able to take full-disk maps of the LOS B-field every 45 seconds. The starting time, t_0, of our selected observation period was on 10-Feb-2011, 00:00:28 UT when the AR 11158 first emerged at heliographic coordinates E53°S20° and the ending time of the period under study was on 16-Feb-2011, 11:18:27 UT when the AR was at W30°S20°, well passed the central meridian. During this six-day-long period, the AR had gone through the emergence phase and fully developed into a mature region. For each of the observation frames, we performed a geometrical correction to get the radial, or normal field B_n, from the LOS magnetograms. For further processing, we selected a cutout of $240'' \times 200''$ with a guiding center following the AR at the Carrington rotation rate. Lastly, we rotated the solar sphere from the center of the cut-outs to the solar disk center, practically eliminating both the solar rotation and the projection effects as well, and resulting in a good alignment of cut-out images. By such pre-processing, we produced a uniform dataset ready to be used in our stacking method.

The image-stacking method works as follows. Each of the frames is a map of the B-field at the (thin) photospheric layer. We proceed on making a stack along the time dimension using a 7.5 minute cadence of the 2-D cutouts. This cadence effectively reduces the number of images by a factor of 10, from 12 330 images to 1233 images over the time period under study. The choice of number of images accommodates the maximum computer capacity in both hardware (in particular, the memory) and the software. By starting with t_0 at the top of the stack (the X and Y dimension) and adding images at later times consecutively at a lower height (the Z dimension), we create a 3D data cube, which effectively reconstructs the 3D magnetic structure of the AR. We believe that such reconstructed 3D field is similar to that below the photospheric surface prior to the emergence of the AR. As a first-order approximation, the velocity of the emergent structure is considered constant, thus each frame contributes equally to the height of the structure. For better showing the emergence structure, we used only ~ 4.4 days worth of data (ending on 14-Feb-2011 04:25:17 UT), i.e. the first 800 images instead of the full processed dataset. The (x, y, z) final dimensions of the datacube are 480 pix $\times$ 400 pix $\times$ 800 pix. The datacube, which is produced in IDL, is imported to PARAVIEW, a visualization software package, for further processing and inspection.

3. Results

3.1. 3D Topology of the AR

In Figure 2, we present the resulted reconstruction by showing the iso-surfaces in the 3-D data-cubes for two representative constant contour values (see online material for a video fly-by around the two iso-surfaces). One contour level is at 1100 G, which shows the “skeleton” of the structure, i.e. the core structures of each sunspot/magnetic element of the AR, and the other one at 400 G, which shows finer structures that envelope the “skeleton” structure of 1100 G. Apparently, the AR is composed of four major magnetic concentrations or polarities, as indicated as P1, N1, P2, N2, respectively in the bottom panel of Figure 2. The same four polarities are marked in panel (c) and (f) in Figure 1. As seen from the 3-D map, the four polarities originate from two bipoles, P1-N1 and P2-N2. Here, we will be using the terms “bipole” or “flux-tube” interchangeably, whenever referring to a certain group of P1-N1 or P2-N2. The positive polarity P1 connects to its corresponding negative polarity N1, and P2 connects to N2. In other words, the pairs P1-N1, P2-N2 form two neighboring flux-tube systems. It is easy to note that P1 and N1, and P2 and N2 are not closing at their apex, since at this location, the field is weak and mostly transverse to the LOS. However, if we go down to lower B-field iso-surfaces, i.e. 400 G, we can clearly see an almost closed system of adjacent branch-like arches.

Instead of coherent, solid flux-tubes, we observe a very fragmented, branch-like appearance in all polarities of the bipoles. On the surface, such fragmentation appeared as the continuous emergence of individual small magnetic elements. However, these small magnetic elements exhibit a remarkably ordered, "swarm"-like collective behavior, separating in terms of polarity and coalescing in 3D into big "tree-trunks" − i.e. the four polarities of the quadrupolar AR. This tree-branch-trunk feature signifies a deeper relation of all the small magnetic features within a large-scale emerging structure. Each polarity consists of several branches, which are almost perfectly connected to the branches in the opposite polarity along the flux-tubes. The branches are probably caused by a bifurcation process which is further discussed below.

3.2. Bifurcation in Height

Both bipoles exhibit similar bifurcation along the height. An inspection on the datacubes reveals that, for each bipole, there seems to be a two-phase evolution − or, equivalently, a "grouping" of the individual small branches to just two −but larger− groups we dub "Mega-Branches" ("Mega-Branch-α" and "Mega-Branch-β" or for short "MBα" and "MBβ", with "MBα" preceding "MBβ" in time, as illustrated in Figure 2). A more thorough study of the magnetic morphology should include the time-flux profile to characterize the temporal evolution in a more quantitative manner as discussed below.

In Figure 3, we show the magnetic flux versus time for each individual polarity of the AR, i.e. P1, N1, P2 and N2, and we overplot each polarity's unsigned profile in the same graph. According to this plot, P1-N1 (solid lines) is the first one that emerges and it is followed by the second bipole, P2-N2, about only six hours later (dashed lines). From the time-flux profile in Fig. 3, we see that for an individual bipole (i.e. N1-P1 and N2-P2) the magnetic flux of its positive and negative polarity is − to a first order − very similar; such similarity is in phase throughout the emergence period. Also, for both bipoles, two major flux-emergence phases are identified, with the initial one being moderate ("MBα") and the later one ("MBβ") being a stronger "flux-surge". The two phases in time are understood as the two adjacent "Mega-branches" of the emerging flux-tube, as suggested by the 3-D reconstruction of Fig. 2. In each of the bipoles, the Mega-Branch that arrives first at the photosphere, "MBα", appears somewhat weaker and fragmented whereas the branch that arrives $\sim$ 2 days later, "MBβ", is much stronger. Like we already mentioned, these flux-surge branches can be grouped as a whole into one "Mega-Branch-β" for each bipole, as also suggested by the Flux vs. time diagram. Thus, for each bipole we have a bifurcation in height.

In Table 1, we provide the total unsigned flux emerged for each Mega-Branch's polarity along with information on the duration of emergence and the flux-emergence rate, as measured from Figure 3. The duration of emergence is the time between the onset (annotated green lines) and the end-of-emergence flux (colored asterisks) for each Mega-Branch. The rate of emergence is defined as the flux measured for each Mega-Branch, divided by its respective duration of emergence. For comparing the individual polarities, we present measurements for MBα+MBβ, i.e. unifying the Mega-Branches by using the onset time of MBα's and for the end time, the one of MBβ's (thus yielding information for the emergence of individual polarities). The AR 11158 is a strong AR where emergence lasted 110 hours with a flux-emergence rate of 5.99×10^{16} Mx s^{-1}, leading to a total emerged unsigned flux of 2.4×10^{22} Mx. Going down to the level of the individual polarities, we should be able to quantify the similarities seen in the 3D visualization. For both bipoles, the MBβ emergence rates are a factor of 3.2 larger as compared to the MBα rates, on average. Furthermore, the onset times for the Mega-Branches of the Bipoles N1-P1/N2-P2 are only $\sim$ 6 hours apart, i.e. very similar as it can be also seen in the 3-D reconstruction of Fig 2.

3.3. Bifurcation in Horizontal Direction

At a first sight, AR 11158's magnetic topology seems rather complex. However, the tendency for collinearity of the four polarities at the bottom of the 3-D cube, suggests that both flux-tubes might be related, even originating from the same parental magnetic flux-tube. This picture is therefore suggesting that a single sub-photospheric flux-tube has been bifurcated into two tubes along the horizontal direction , as illustrated in Figure 4. If the two flux-tubes had independent origin, it would be difficult to understand why they became more aligned at a later evolution stage than at the earlier phase. The almost in-phase evolution of the fluxes with time of the two bipoles further reinforces this interpretation.

Flux tubes are non-planar when they first emerge through the quiet sun (see Fig 1 and the online videos). However, right before the emergence of the "flux-surge" in both of the bipoles, there is a strong pushing-aside of the already emergent Mega-Branches ("MBα's") in a manner like they seem to "know in advance" about the arrival of the stronger "flux-surge" tubes (or "MBβ's"), suggesting that the "MBβ's" interact/collide sub-photospherically with the trunks of the "MBα" tubes. At a later time, i.e. at the bottom of the data-cube, the polarities assume the "correct", Joy's law-compliant tilt. In strong flux emergence events, the observed separation of polarities and the magnetic flux build-up usually don't last more than 3 days (Fan 2009).

Further, for each bipole, the asymmetric polarity separation suggests flux-tubes with an oblique Λ-shape instead of axisymmetric Ω-loops. The Λ-shape has its leading leg more tilted away from the vertical direction than the trailing leg. This asymmetry can be understood in terms of the Coriolis force acting on a rising flux-tube, as discussed by Caligari et al. (1995) with the TFT approximation and also reproduced using anelastic MHD models (Abbett et al. 2001).

4. Discussion and Conclusion

In this letter, we presented a novel image-stacking technique for reconstructing the 3-D structure of buoyant flux-tubes rising through the solar surface and forming observed solar active regions. Sequences of images have been used before to infer the structure of ARs , e.g. observational inferences on the nature of delta-configuration ARs by Tanaka (1991) . Leka et al. (1996) used a similar stacking method to demonstrate the twist in emerging ARs and found evidence that they carry electrical currents before they emerge. However, the previous attempts are limited to track the locations of AR centroids with time, but not the entire structure. To our best knowledge, this work is probably the first true implementation of the image-stacking technique to reconstruct the detailed 3-D structure of an AR, using advanced visualization software and high cadence high resolution magnetogram data.

At least in the early stages of emergence, the emerging magnetic structures are two non-planar neighboring bipoles, but a more detailed picture reveals a bifurcated structure for both bipoles, in the horizontal direction and along the height as well. In the low B-field iso-surfaces, multiple magnetic arches can be observed to emerge in a continuous manner, with the like-polarities coalescing with time. The 3-D reconstruction provided good evidence that Mega-branches could be originating from the same flux-tube below the photosphere. Last, we find that there's a dual-phase evolution for both bipoles, as suggested by both the topology in 3D and the time-flux profile of the AR, providing further evidence for a bifurcation in height. Observations also indicate that the two bipoles have a common origin. The two bipoles have a similar topology in 3-D, similar temporal evolution in flux emergence, and most significantly, appear almost collinear at the later stage of emergence. It is possible that the two bipoles are the result of bifurcation of a single progenitor flux tube early in the evolution.

It is interesting to note that the 3-D morphology of the AR 11158 −for each bipole as well as overall− exhibits all the qualitative characteristics of the TFT approximation. The TFT model's successes in reproducing observations qualitatively are well known (Caligari et al. 1995). The same qualitative characteristics of the TFT were reproduced in incompressible MHD simulations by Abbett et al. 2001 by including the Coriolis force due to the solar rotation, in order to study its effects on the fragmentation of flux-tubes. This simulation reproduces the non-axisymmetrical morphology that arises due to the Coriolis force. From our reconstruction it is evident that we have such an asymmetry. The fact that we observe it, is suggesting that the upper SCZ has not a severe impact in altering the magnetic morphology of flux-tubes while transversing the lower convection zone, after they are born. Also, the large initial horizontal separation of the two bipoles may have happened deep in the SCZ as it is hard to imagine the non-axisymmetrical morphology that both bipoles possess, to happen at heights close to the surface, since this is readily explained by the act of Coriolis force throughout the journey of the tubes in the SCZ. Thus, we conclude that the horizontal bifurcations may have happened at an early stage in each tube's evolution. However, the small arch-like magnetic "fibers" seen in the 400 G isosurfaces may be caused by the large pressure gradient in the upper convection zone.

This study also demonstrates that the image-stacking technique is a promising method for studying the 3D structure of ARs prior to their emergence. In the future, we will study the magnetic vector 3-D structure by fully using the magnetic vector observations from the SDO/HMI instrument.

The authors wish to thank Drs. M. Linton, Y. Fan and M.K. Georgoulis for valuable discussions. G. Chintzoglou also thanks Prof. C.E. Alissandrakis for inspiring conversation and encouragement. We acknowledge the support from NSF ATM-0748003, NSF AGS-1156120. One of the authors (G.C.) was supported by NASA Headquarters under the NASA Earth and Space Science Fellowship Program - Grant NNX12AL73H.

REFERENCES

Abbett, W. P., Fisher, G. H., & Fan, Y. 2001, ApJ, 546, 1194

Caligari, P., Moreno-Insertis, F., & Schussler, M. 1995, ApJ, 441, 886

Charbonneau, P. 2005, Living Reviews in Solar Physics, 2, 2

Cheung, M. C. M., Rempel, M., Title, A. M., & Schüssler, M. 2010, ApJ, 720, 233

Fan, Y. 2008, ApJ, 676, 680

—. 2009, Living Reviews in Solar Physics, 6, 4

Gough, D. O. 1969, Journal of Atmospheric Sciences, 26, 448

Hale, G. E., Ellerman, F., Nicholson, S. B., & Joy, A. H. 1919, ApJ, 49, 153

Leka, K. D., Canfield, R. C., McClymont, A. N., & van Driel-Gesztelyi, L. 1996, ApJ, 462, 547

Schou, J., Scherrer, P. H., Bush, R. I., et al. 2012, Sol. Phys., 275, 229

Spruit, H. C. 1981, A&A, 98, 155

Stein, R. F. 2012, Living Reviews in Solar Physics, 9, 4

Strous, L. H., Scharmer, G., Tarbell, T. D., Title, A. M., & Zwaan, C. 1996, A&A, 306, 947

Strous, L. H., & Zwaan, C. 1999, ApJ, 527, 435

Sun, X., Hoeksema, J. T., Liu, Y., et al. 2012, ApJ, 748, 77

Tanaka, K. 1991, Sol. Phys., 136, 133

Zwaan, C. 1987, ARA&A, 25, 83

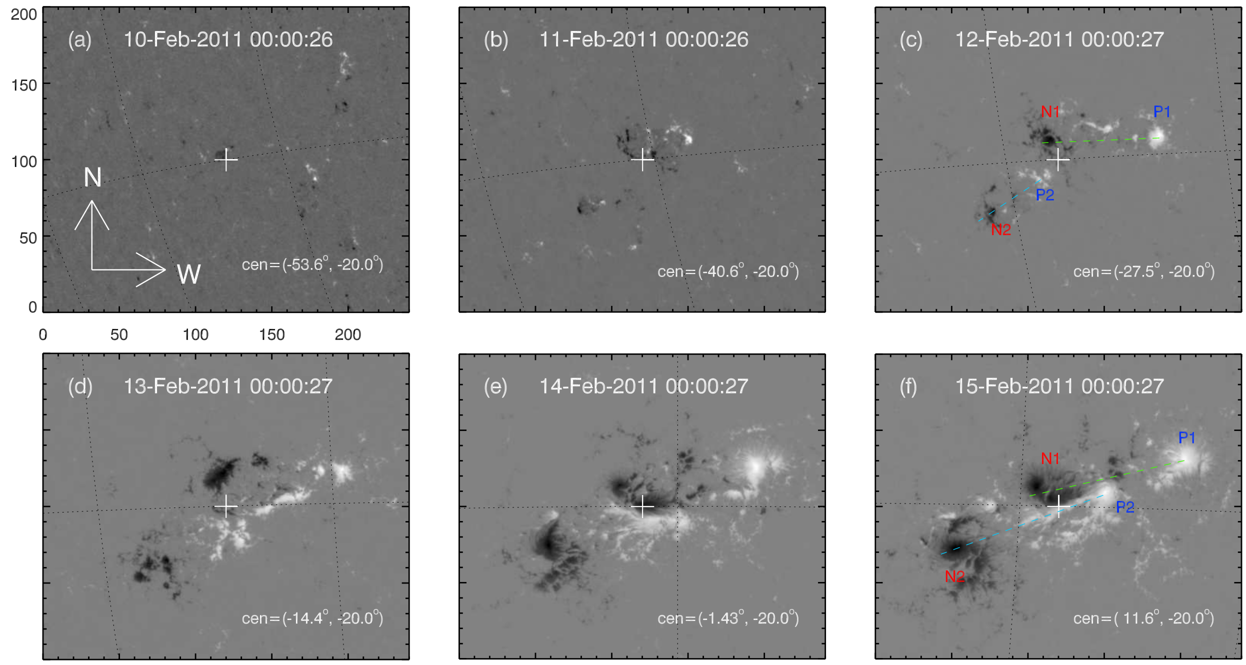

Fig. 1.— The first six days of evolution of the AR 11158 as observed with the SDO/HMI LOS magnetograph. The individual polarities are named after which bipole emerged first, e.g. bipole 1, hence we name its negative polarity N1 and its positive P1, and with N2 and P2 emerging at a later time. The white cross shows the position of the guiding center of the $240'' \times 200''$ FOV at a fixed heliographic latitude $\phi = -20°$. Note that the bipoles initially are non-collinear (dashed lines, panel (c)); at a later time they become quasi-collinear (panel (f)).

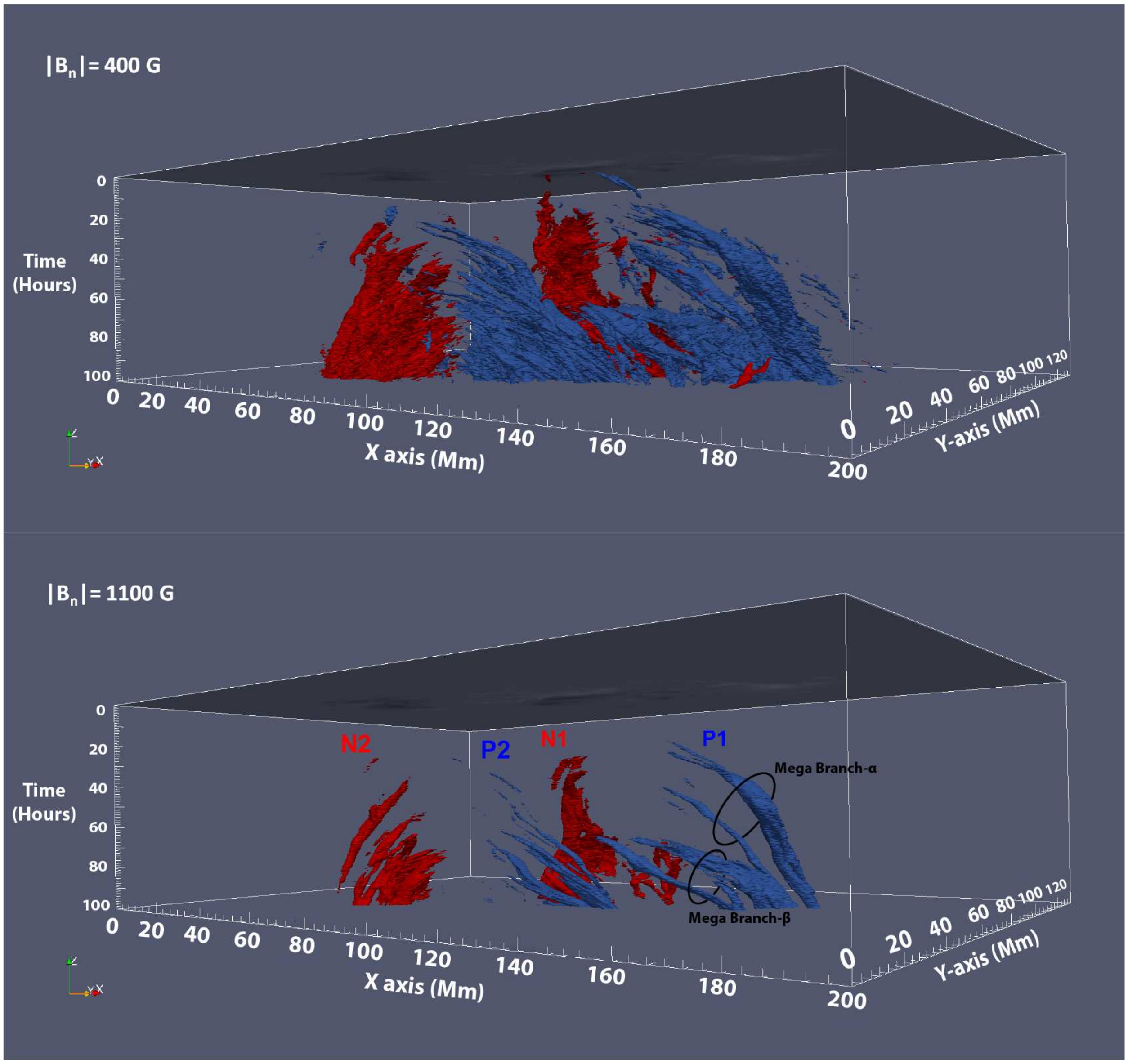

Fig. 2.— The 3-D reconstruction of AR 11158 using the image-stacking method on SDO/HMI LOS magnetograms. The flux-tubes shown here are at $|B_n| = 400$ G (up) and 1100 G (down). On top of each datacube is the last HMI LOS frame of the cube, i.e. the bottom frame, on 14-Feb-2011 04:25:57. The presented duration of the observation is 100.4 hours. The positive X-axis direction is westward and Y-axis northward. The length of the X-axis is roughly comparable with the height of the Solar Convection Zone (SCZ), i.e. about 200 Mm.

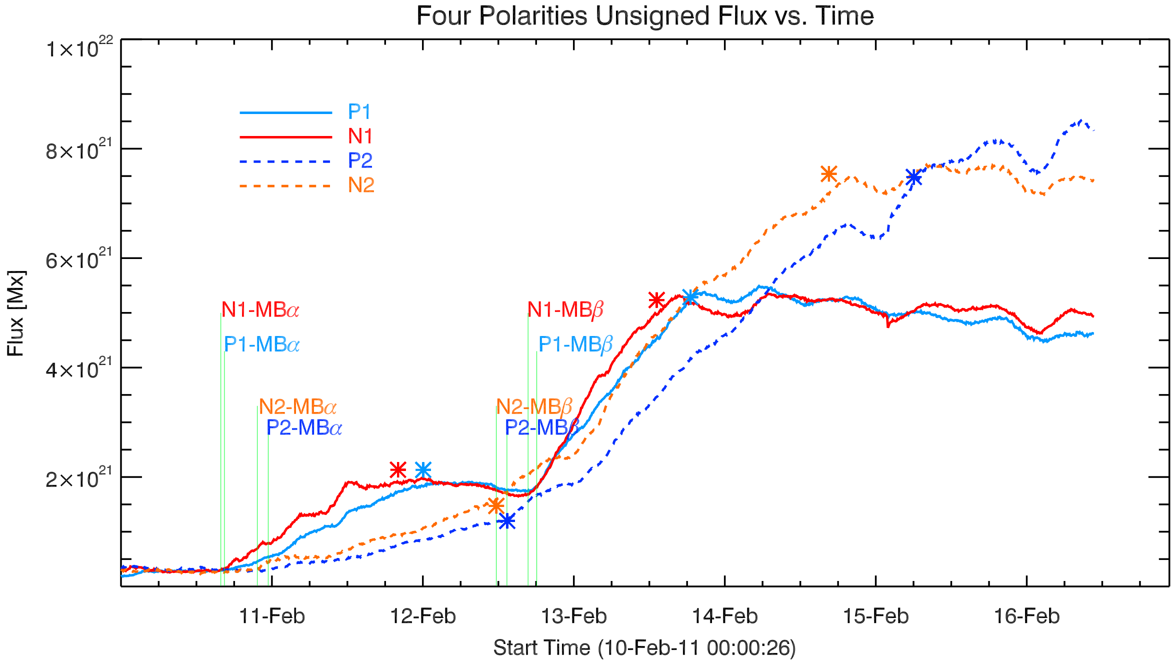

Fig. 3.— The time evolution of the flux for the bipoles N1-P1 (solid lines) and N2-P2 (dashed) suggests that both have an early emergence phase (i.e. "MBα") or "front" of flux, followed by a strong flux "surge" (or "MBβ") as also can be seen in Fig 2. Note the persistent lagging of the positive, i.e. leading polarities, P1 and P2 with respect to the following N1 and N2. The green lines denote the onset of emergence events. Also, for each Mega-Branch, the end of emergence is shown with an asterisk (*) in the respective color.

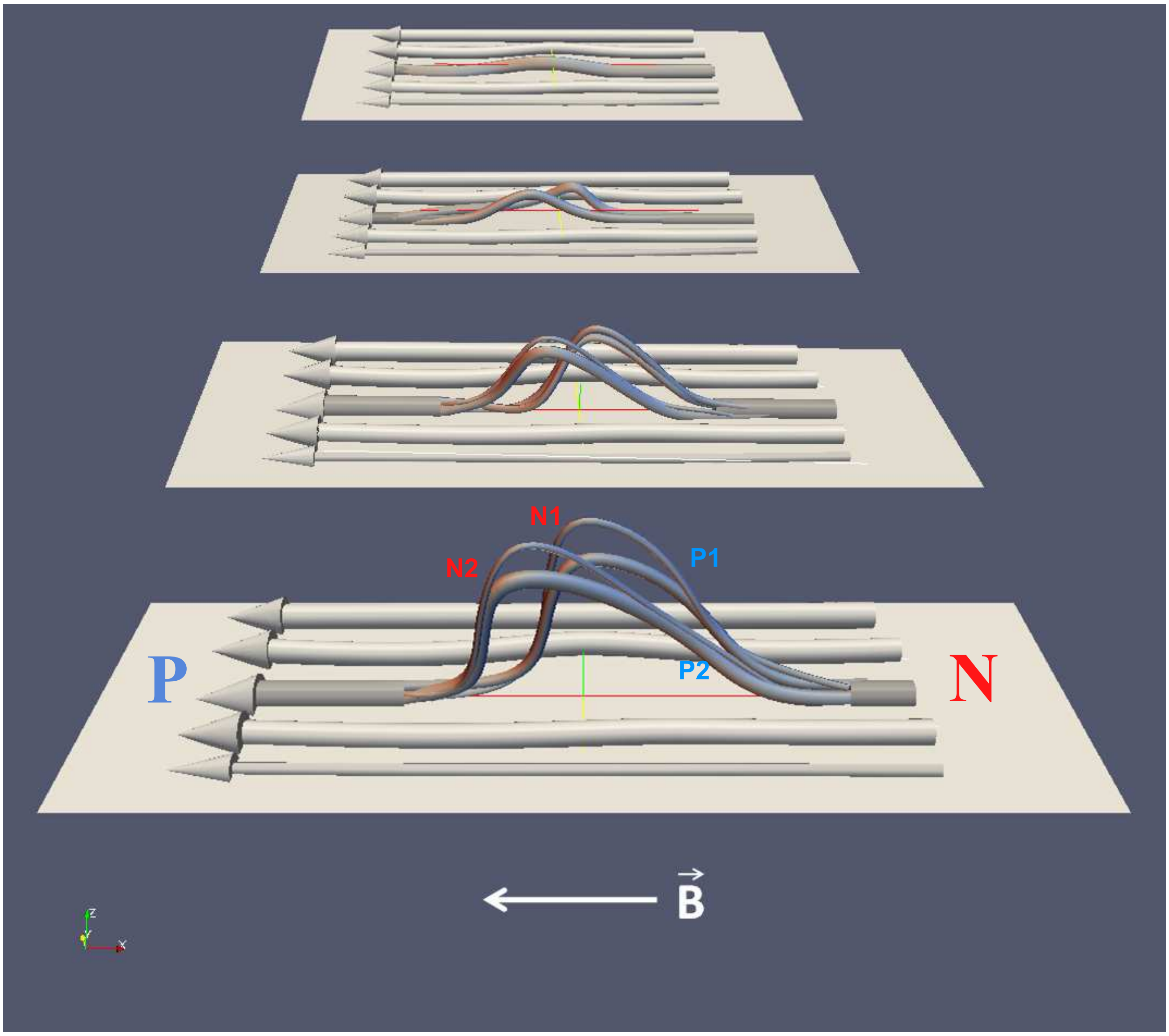

Fig. 4.— Model sketch of the emergence process of AR 11158 in the sub-photosphere. The plane is at the depth of the bottom of the SCZ that B-fields originally reside. The cylindrical structures shown at that plane in the SCZ are the flux-tubes of the toroidal field, generated by the solar dynamo process. For flux-tubes created in the South hemisphere during Solar Cycle 24 (like AR 11158), the B-field vector along the tubes is directed from West-to-East (here from right-to-left), as dictated by Hale's law of polarity and the Babcock-Leighton dynamo theory. The flux-tubes also develop an asymmetric lambda shape ("Λ") as they rise.

Table 1. Flux Emergence Rate, Total Flux Emerged and Duration of Emergence

Bipole	Polarity	Mega-Branch	Rate[a]	Total[b]	Start Time	End Time	Duration[c]
1	P1	MBα	1.33	1.52	10-Feb 16:27	12-Feb 00:00	31.66
		MBβ	3.87	3.41	12-Feb 18:06	13-Feb 18:30	24.50
		MBα+MBβ	1.85	4.93	10-Feb 16:27	13-Feb 18:30	74.15
	N1	MBα	1.57	1.59	10-Feb 15:52	11-Feb 20:03	28.16
		MBβ	4.43	3.27	12-Feb 16:31	13-Feb 13:10	20.50
		MBα+MBβ	1.87	4.66	10-Feb 15:52	13-Feb 13:10	69.28
2	P2	MBα	0.67	0.91	10-Feb 23:24	12-Feb 13:21	37.99
		MBβ	2.64	6.15	12-Feb 13:21	15-Feb 06:00	64.64
		MBα+MBβ	1.91	7.06	10-Feb 23:24	15-Feb 06:00	102.63
	N2	MBα	0.91	1.24	10-Feb 21:40	12-Feb 11:40	38.00
		MBβ	2.94	5.59	12-Feb 11:40	14-Feb 16:30	52.87
		MBα+MBβ	2.09	6.83	10-Feb 21:40	14-Feb 16:30	90.88
1+2			5.99	23.79	10-Feb 15:52	15-Feb 06:00	110.16

[a] $\times 10^{16}$ Mx s^{-1}

[b] $\times 10^{21}$ Mx

[c] hours